Investigation into the radiobiological consequences of pre-treatment verification imaging with megavoltage X-rays in radiotherapy

BJR

Received:
29 November 2013

Revised:
22 January 2014

Accepted:
23 January 2014

doi: 10.1259/bjr.20130781

Cite this article as:
Hyland WB, McMahon SJ, Butterworth KT, Cole AJ, King RB, Redmond KM, et al. Investigation into the radiobiological consequences of pre-treatment verification imaging with megavoltage X-rays in radiotherapy. Br J Radiol 2014;87:20130781.

FULL PAPER

Investigation into the radiobiological consequences of pre-treatment verification imaging with megavoltage X-rays in radiotherapy

[1]W B HYLAND, PhD, [2]S J MCMAHON, PhD, [2]K T BUTTERWORTH, PhD, [2,3]A J COLE, MB BCh, MRCP, [1]R B KING, PhD, [2]K M REDMOND, PhD, [2]K M PRISE, PhD, [1,2]A R HOUNSELL, PhD and [1,2]C K MCGARRY, PhD

[1]Radiotherapy Physics, Northern Ireland Cancer Centre, Belfast Health and Social Care Trust, UK
[2]Centre for Cancer Research and Cell Biology, Queen's University Belfast, Belfast, UK
[3]Clinical Oncology, Northern Ireland Cancer Centre, Belfast Health and Social Care Trust, UK

Address correspondence to: Dr Wendy Bridget Hyland
E-mail: *wendy.hyland@belfasttrust.hscni.net*

Objective: The aim of this study was to investigate the effect of pre-treatment verification imaging with megavoltage X-rays on cancer and normal cell survival *in vitro* and to compare the findings with theoretically modelled data. Since the dose received from pre-treatment imaging can be significant, the incorporation of this dose at the planning stage of treatment has been suggested.
Methods: The impact of imaging dose incorporation on cell survival was investigated by clonogenic assay of irradiated DU-145 prostate cancer, H460 non-small-cell lung cancer and AGO-1522b normal tissue fibroblast cells. Clinically relevant imaging-to-treatment times of 7.5 and 15 min were chosen for this study. The theoretical magnitude of the loss of radiobiological efficacy due to sublethal damage repair was investigated using the Lea–Catcheside dose protraction factor model.
Results: For the cell lines investigated, the experimental data showed that imaging dose incorporation had no significant impact on cell survival. These findings were in close agreement with theoretical results.
Conclusion: For the conditions investigated, the results suggest that allowance for the imaging dose at the planning stage of treatment should not adversely affect treatment efficacy.
Advances in knowledge: There is a paucity of data in the literature on imaging effects in radiotherapy. This article presents a systematic study of imaging dose effects on cancer and normal cell survival, providing both theoretical and experimental evidence for clinically relevant imaging doses and imaging-to-treatment times. The data provide a firm foundation for further study into this highly relevant area of research.

Radiotherapy is in a period of rapid scientific and clinical development. With the introduction of adaptive radiotherapy[1] and the increasing use of high-precision techniques,[2] there has been an increased requirement for verification imaging. Verification imaging can be carried out using megavoltage portal beams, kilovoltage planar fields or cone beam CT (CBCT) using kilovoltage or megavoltage beams. Dependent on the imaging technique employed, the dose required to acquire an image of adequate quality can vary significantly. Whilst doses ranging from a few centigrays to 10 cGy are required for megavoltage portal imaging and CBCT, doses in the order of megagrays are typically required to obtain an image of adequate quality using kilovoltage planar imaging.[3] The choice of imaging modality is dictated by the available technology, with megavoltage portal imaging being the most established imaging option. However, with the addition of on-board kilovoltage imaging systems, kilovoltage imaging options are becoming much more widespread both for their improved image contrast and reduced patient dose.[4]

Associated with this increasing imaging dose burden are concerns regarding the increased risk of deterministic and stochastic effects due to increased radiation exposure.[3,5–7] Whilst it is important to quantitatively determine the long-term effects of increased concomitant exposures, it is equally important to determine any potential changes to the effectiveness of the therapeutic dose.[5,8–10]

Low-dose biological phenomena such as adaptive responses[11–13] and bystander signalling[14–17] hold the potential to significantly alter the response of cells to radiation and thus treatment efficacy. However, since these effects tend to occur over a period of hours, it is unlikely that they will have any significant impact with regard to imaging in the

Table 1. Average imaging-to-treatment times (τ_{I-T}) and overall treatment times (OTT) determined from a clinical audit of 30 prostate and pelvic node intensity-modulated radiotherapy (IMRT) patients and 30 prostate three-dimensional conformal radiotherapy (3DCRT) patients

Treatment type	$\tau_{I-T} \pm$ SD (min)	Upper 95% CI (τ_{I-T})	OTT $\pm$ SD (min)	Upper 95% CI (OTT)
IMRT	8.56 $\pm$ 3.62	15.67	14.93 $\pm$ 4.4	23.55
3DCRT	8.18 $\pm$ 5.25	18.48	11.48 $\pm$ 5.62	22.48

CI, confidence interval; SD, standard deviation associated with the calculated values.

treatment room.[18] By contrast, sublethal damage repair that can occur over a period of minutes may be of significance in radiotherapy when the dose delivered from imaging beams is incorporated with the prescribed therapeutic dose at the treatment planning stage.[9,10,19–22]

The effect of imaging dose incorporation was previously reported in a preliminary study by Yang et al.[10] In particular, they showed an unexpected 12.6% increase in cell survival when H460 cells were exposed to a pre-treatment imaging dose of 5 cGy followed by a therapeutic dose of 200 cGy, they attributed

Figure 1. (a) An image of the irradiation set-up. (b) A schematic representation of the experimental set-up. The cells were irradiated at 4.8 cm deep in a custom-made polymethyl methacrylate phantom, with 5 cm of backscatter. (Inset) the dose profile across the three flasks at the cell level, acquired using a two-dimensional matrix ion chamber array at an effective depth of 5 cm.

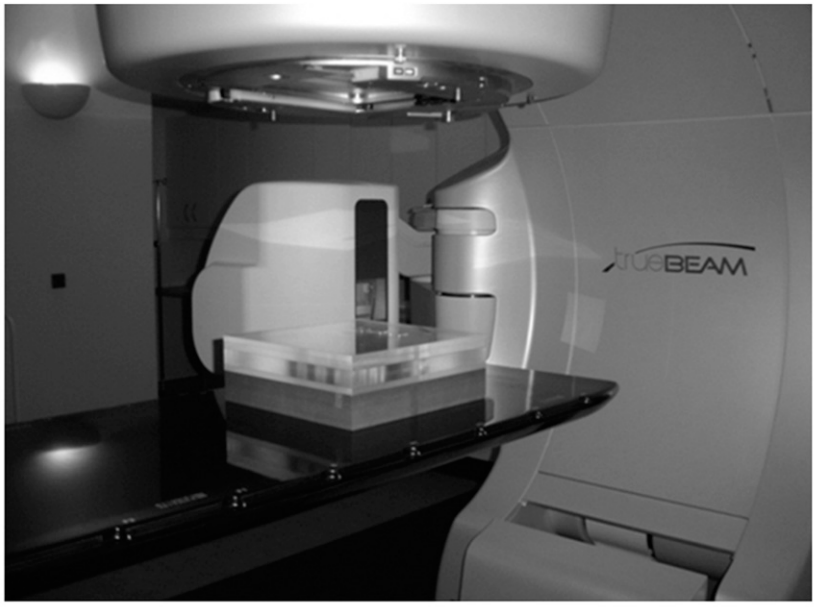

(a)

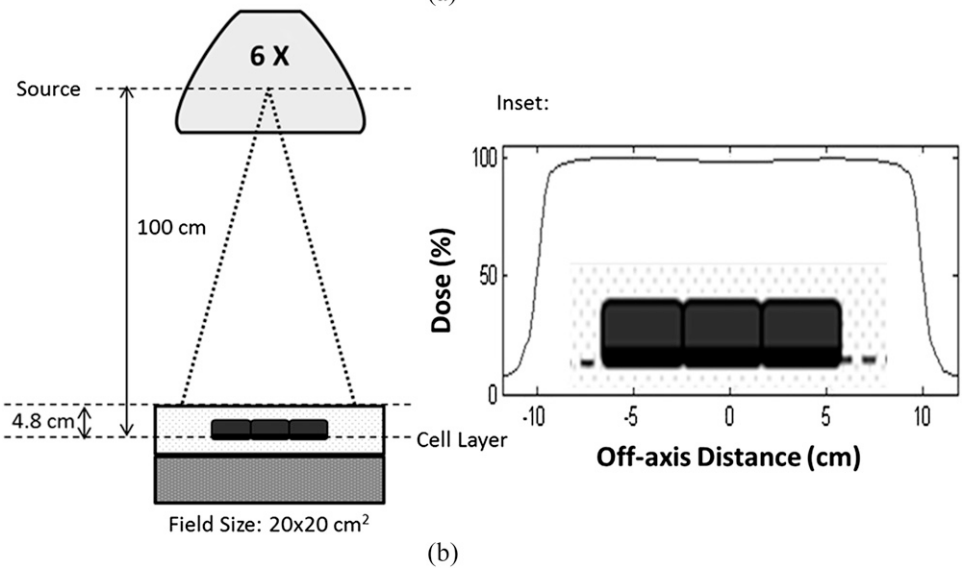

(b)

their findings to increased cell proliferation. The results suggest that the delivery of a fraction of the therapeutic dose by imaging beams presents a potential issue since the time from imaging to delivery of the treatment can be of the order of 5–20 min, having a negative impact on treatment efficacy owing to low-dose biological phenomena[16] or sublethal damage repair that may be initiated during this time.[9,19] Although the need for imaging dose incorporation is justified, the potential to affect treatment efficacy should be determined.

To investigate the radiobiological impact of imaging dose incorporation, a series of experiments were conducted *in vitro*, where the imaging doses were incorporated with the prescribed treatment dose for different human cell lines. As megavoltage portal imaging is the most widely used type of imaging for verification and as it delivers a higher dose, the study was carried out using 6 MV beams for both the imaging and treatment components. The theoretical magnitude of this effect and its impact on cell survival was quantified using radiobiological modelling based on the Lea–Catcheside dose protraction factor[23] as a comparison to the experimental data.

METHODS AND MATERIALS

Clinical audit

Using the Varian offline review program (Varian Medical Systems, Inc., Palo Alto, CA), an analysis of the time taken between the acquisition of a pre-treatment verification image and the treatment delivery was carried out for 30 patients for prostate and pelvic node intensity-modulated radiotherapy (IMRT) and 30 prostate patients for three-dimensional conformal radiotherapy (3DCRT), who were undergoing treatment at the Northern Ireland Cancer Centre (Belfast, UK). The time between the acquisition of the first megavoltage portal image and treatment was recorded (τ_{I-T}), as was the overall treatment time (the average time from the acquisition of the first megavoltage portal image to the end of the treatment). The results are presented in Table 1. For the IMRT and 3DCRT patient groups, a total of 106 and 101 treatment fractions were analysed, respectively. From these data, image-to-treatment times (τ_{I-T}) of 7.5 and 15 min were chosen for this study, as they were considered to be broadly representative of the average and upper extreme values of this data set. These values are consistent with typical imaging-to-treatment times of 5–20 min that have been reported previously.[9]

Cell culture

Experiments were conducted using the human prostate cancer cell line DU-145 and the human non-small-cell lung cancer cell line H460, obtained from the American Type Culture Collection LGC Standards (Teddington, UK). Both cancer cell lines were grown in RPMI-1640 with L-glutamine (Lonza, Cambridge, UK), supplemented with 10% foetal bovine serum and 1% penicillin/streptomycin (Gibco®, Paisley, UK). The human tissue fibroblast cell line (AG0-1522b) cells were purchased from the Coriell

Figure 2. A schematic representation of the experimental design. The standard group received the prescribed dose (D_T) in a single irradiation, delivered at 400 MU min^{-1} ($\dot{D}_T$); while the split-dose group received the prescribed dose in two time-separated irradiations —5 cGy (D_I) at a dose rate of 100 MU min^{-1} ($\dot{D}_I$) followed by the remainder of the total dose prescribed at a dose rate of 400 MU min^{-1}. Time between delivery of the pre-treatment imaging dose and the remainder of the total dose prescribed (τ_{I-T}) was either 7.5 or 15 min. $\triangle t_I$, time taken to deliver the imaging beam; $\triangle t_T$, time taken to deliver the treatment beam; t_{start}, start time; t_{stop}, stop time.

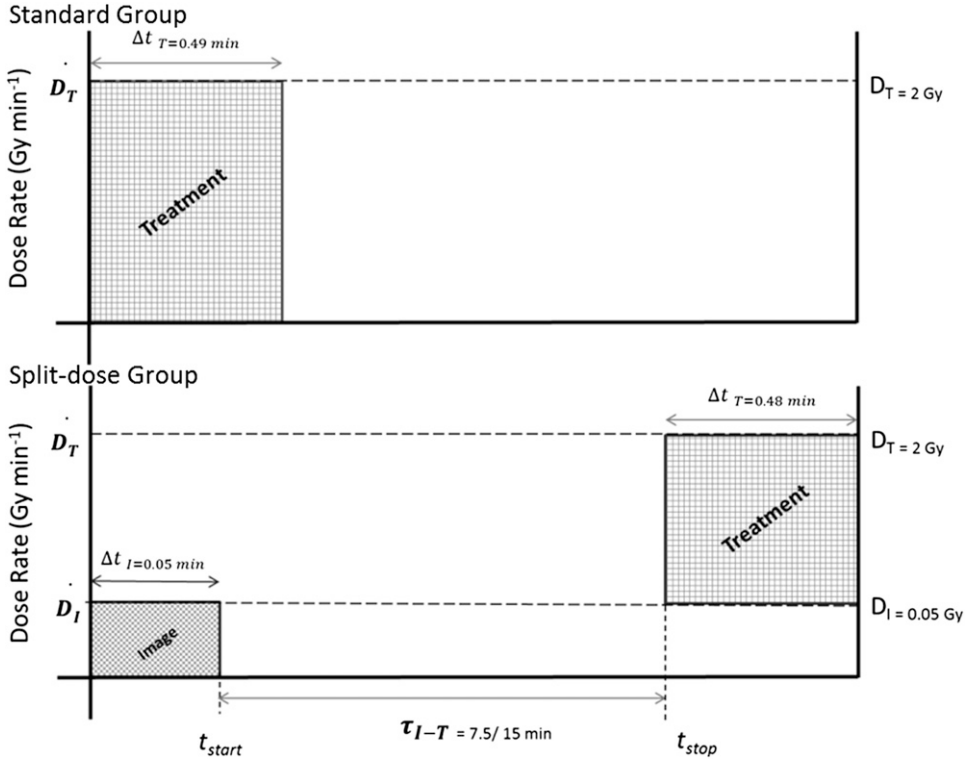

Institute for Medical Research (Camden, NJ) and grown in Eagle's minimum essential medium with deoxyribonucleosides and deoxyribonucleotides (Lonza), supplemented with 20% foetal bovine serum and 1% penicillin/streptomycin. All cell lines were maintained at 37 °C in an atmosphere of 5% CO_2 in air and 95% humidity.

Clonogenic assay

The effect of radiation on cell viability was investigated using the clonogenic assay.[24] All cells were plated 18–24 h prior to exposure. The DU-145 and H460 cells received doses of 2, 4 or 8 Gy, whereas the more radiosensitive AGO-1522b cells received doses of 1, 2 or 4 Gy. Prior to irradiation, the culture flasks were completely filled with RPMI-1640 incomplete media to ensure full scatter conditions. Irradiations were conducted at room temperature (25 ± 2 °C). All exposures were conducted in triplicate on at least three independent occasions. For all experiments, six unexposed controls were prepared and sham irradiated. After exposure, the incomplete media was removed from the flasks and replaced with 5 ml of RPMI-1640 complete media. The cells were subsequently incubated for 8–12 days at 37 °C, in an atmosphere of 5% CO_2 in air and 95% humidity. At the appropriate time, the cells were stained with 0.5% crystal violet in 50% methanol. Cell colonies were scored manually using the 50-cell exclusion criterion.

Irradiation set-up and *in vivo* experimental design

A monolayer of cells was irradiated in T25 culture flasks with 6 MV X-rays produced by a TrueBeam™ LINAC (Varian Medical Systems, Inc.) under a uniform beam (Figure 1a). Three T25 flasks were irradiated simultaneously. The cells were separated by a distance of 100 cm from the X-ray source, for a field size of 20 × 20 cm (at 100 cm). A schematic representation of the experimental set-up is shown in Figure 1b.

Investigations were conducted to determine the effect of combining a pre-treatment imaging dose of 5 cGy[25] with a variable therapeutic dose to deliver total doses of 2, 4 or 8 Gy for DU-145 and H460 cells or 1, 2 or 4 Gy for the AGO-1552b cells. The delivery of the two parts of the total dose was separated by times of 7.5 or 15 min. Standard dose–response curves of cell survival were also generated for each data set as a comparison. Figure 2 shows a schematic representation of the two irradiation groups—standard and split dose. The standard group received the prescribed dose (D_T) in a single irradiation, delivered at 400 monitor units (MU) min^{-1}; whereas, the split-dose group received the prescribed dose in two time-delayed irradiations. Specifically, the first irradiation delivered a dose of 5 cGy at 100 MU min^{-1} to the cells (representing a pre-treatment imaging dose) and the second irradiation delivered the remainder of the total dose prescribed, at a dose rate of 400 MU min^{-1}.

Dosimetric verification

Dosimetry measurements were performed using a Farmer® ionization chamber (NE-Technology Ltd, Reading, UK) at a radiological equivalent depth to the cell position with a calibration traceable to the National Physical Laboratory, in accordance with the Institute of Physical Sciences in Medicine 1990 code of practice.[26] As a further verification of the ionization chamber measurements, a series of CT images of the polymethyl methacrylate phantom containing the culture flasks were taken with a GE LightSpeed® CT scanner (GE Healthcare, Chalfont St Giles, UK). The CT data set was sent from the CT scanner to the Eclipse™ (Varian Medical Systems, Inc.) treatment planning system where the prescription point was positioned at the cell level, at the centre of the middle flask and a 6 MV 20 × 20 cm^2 field planned to deliver a prescription dose of 2 Gy. The number of monitor units required to deliver the prescribed dose was found to be in agreement with the dose determined using the ionization chamber reading to within ±1%. The dose variation between the three flasks irradiated at the same time was <1%.

Experimental data analyses

The fraction of cells surviving after treatment was calculated as the ratio of the number of colonies in the exposed flask to the number of cells seeded, corrected for the plating efficiency of the sham-irradiated controls. The standard error associated with each data point was calculated. The data were subsequently plotted using Origin Pro v. 8 (Origin Lab, Northampton, MA) and fitted to the linear quadratic equation for single acute doses: surviving fraction $= e^{-(\alpha D + \beta D^2)}$, where D is the total dose and α and β are tissue-specific parameters. The fits were weighted by 1/(variance of each data point). F-tests were carried out to determine if any differences in the fits to the data sets were

Table 2. Parameter definition and values used to determine the dose protraction factor $\{G[\dot{D}_{I \text{ and } T}(t)]\}$

Symbol	Definition	DU-145	H460	AGO-1522b
Δt_I	Imaging time	–	–	–
Δt_T	Treatment time	–	–	–
D_T	Total dose (Gy)	2, 4 or 8	2, 4 or 8	1, 2 or 4
D_I	Imaging dose (Gy)	0.05	0.05	0.05
$\dot{D}_T$	Therapeutic dose rate (Gy min^{-1})	4	4	4
$\dot{D}_I$	Imaging dose rate (Gy min^{-1})	1	1	1
$R_{1/2}$	Repair half-time (min)	16	90	130
τ_{I-T}	Imaging-to-treatment time (min)	7.5 or 15	7.5 or 15	7.5 or 15

statistically significant. Statistical significance was assumed for $p < 0.05$.

Modelling the dose protraction

The effectiveness of a prescribed dose of radiation was calculated[9] when it was part delivered by a 6 MV imaging beam (100 MU min^{-1}), either 7.5 or 15 min prior to delivery of the remainder of the prescribed dose by a 6 MV treatment beam (400 MU min^{-1}). By integration of the Lea–Catcheside dose protraction factor $\{G[\dot{D}(t)]\}$,[23] which is based on an assumed mono-exponential pattern of sublethal damage recovery and takes account of the imaging and treatment doses, the protracted exposure time and the time gap between imaging and treatment delivery, the following Equation (1) is obtained:

$$G\left[\dot{D}_{\mathrm{I\ and\ T}}(t)\right] = \frac{1}{\left(\dot{D}_{\mathrm{I}}\Delta t_{\mathrm{I}} + \dot{D}_{\mathrm{T}}\Delta t_{\mathrm{T}}\right)^2}\left[\left(\dot{D}_{\mathrm{I}}\Delta t_{\mathrm{I}}\right)^2 g(\mu\Delta t_{\mathrm{I}}) + \frac{2\dot{D}_{\mathrm{I}}\dot{D}_{\mathrm{T}}}{\mu^2}e^{-\mu\tau_{\mathrm{I-T}}}\left(1-e^{-\mu\Delta t_{\mathrm{I}}}\right)\left(1-e^{-\mu\Delta t_{\mathrm{T}}}\right) + \left(\dot{D}_{\mathrm{T}}\Delta t_{\mathrm{T}}\right)^2 g(\mu\Delta t_{\mathrm{T}})\right] \quad (1)$$

Where $\mu = \ln(2)/R_{1/2}$ and $(\mu\Delta t_{\mathrm{p}}) = 2\mu\Delta t_{\mathrm{p}} + e^{-\mu\Delta t_{\mathrm{p}}} - 1/(\mu\Delta t_{\mathrm{p}})^2$, where Δt_{p} is the duration of the exposure. The definitions of the individual parameters contained within this equation are presented in Table 2. Using the experimentally determined α and β values for each cell line, the calculated dose protraction factor (G) was subsequently incorporated into the linear quadratic model [Surviving fraction $= e^{-(\alpha D + G\beta D^2)}$] to calculate cell survival. From the modelled data of cell survival, an effective dose was then calculated to determine the dose required to achieve the same level of cell kill if the dose was delivered in a single fraction.

RESULTS

Experimental data

Figure 3 shows the survival curves generated for DU-145, H460 and AGO-1552b cells for the standard-dose, split-dose ($\tau_{\mathrm{I-T}}$) = 7.5 min and split-dose $\tau_{\mathrm{I-T}} = 15$ min cases. The determined α and β values for each cell line for each combination of irradiation conditions are presented in Table 3. Analysis did not show any statistically significant differences between the control curve *vs* the 7.5-min split-dose curve for each cell line (DU-145, $p = 0.53$; H460, $p = 0.32$; AGO-1552b, $p = 0.35$) or the control curve *vs* the 15-min split-dose curve (DU-145, $p = 0.39$; H460, $p = 0.27$, AGO-1552b, $p = 0.37$). Moreover, no significant differences were found between the 7.5- and 15-min split dose curves (DU-145, $p = 0.58$; H460, $p = 0.28$; AGO-1552b, $p = 0.36$).

Theoretical data

The dose protraction factors $\{G[\dot{D}_{\mathrm{I\ and\ T}}(t)]\}$ were calculated for each dose and each imaging-to-treatment times investigated for the DU-145, H460 and AGO-1552b cells. The parameter values used to calculate $G[\dot{D}_{\mathrm{I\ and\ T}}(t)]$ are presented in Table 2. Taken from the literature, repair half-times of 16, 90 and 130 min were used for DU-145, H460 and AGO-1552b cells, respectively.[21,27,28] The calculated values were incorporated into the linear quadratic model to calculate the corresponding surviving fractions. The

Figure 3. Cell survival curves following exposure to 6 MV beams delivered either as a standard treatment at 400 MU min^{-1} (circles) or as a split-dose (5 cGy imaging dose at 100 MU min^{-1} and treatment dose at 400 MU min^{-1}) with imaging-to-treatment times = 7.5 (triangles) or 15 min (squares) for (a) DU-145, (b) H460 and (c) AGO-1522b cells. The error bars on the data points represent ± standard error of the mean. Only fits to the standard treatment data are plotted for each cell line.

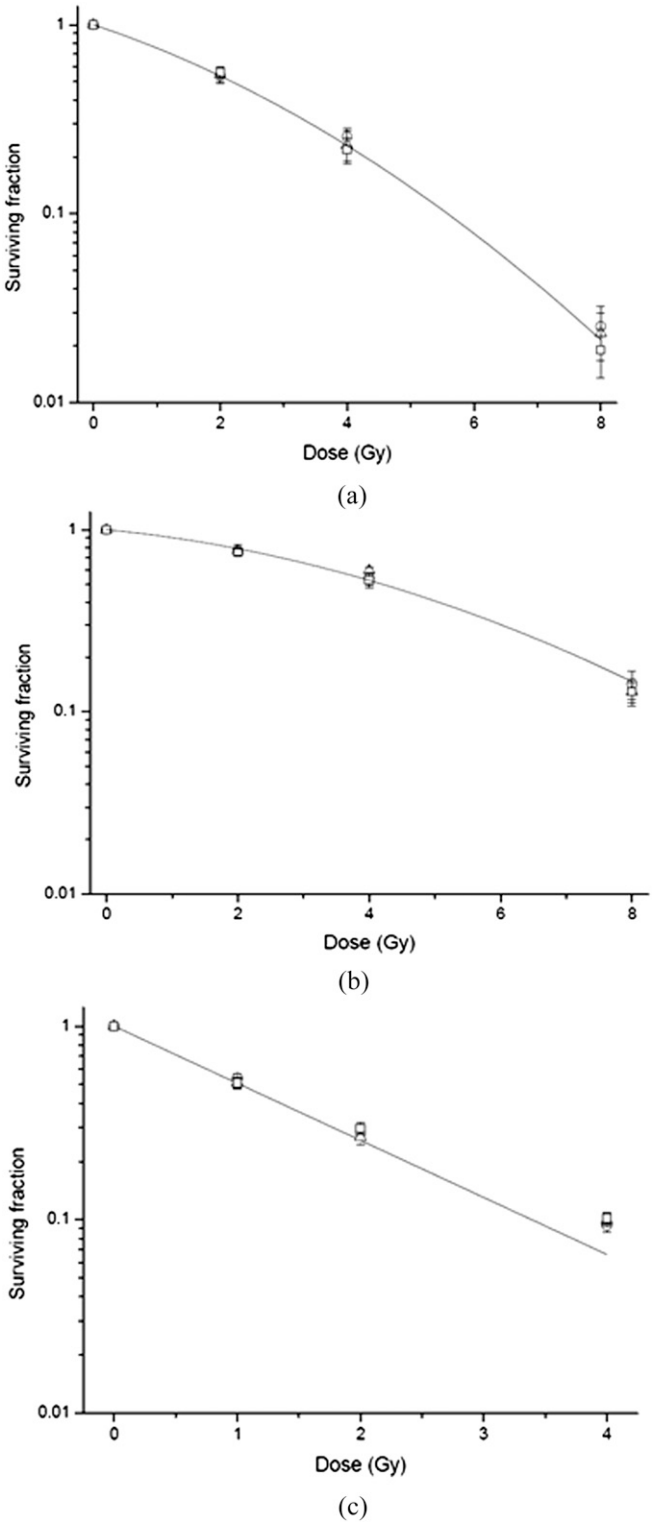

Table 3. Calculated α and β values for the three cell lines investigated

Experimental group	DU-145		H460		AGO-1552b	
	α	β	α	β	α	β
Control	0.08 ± 0.04	0.02 ± 0.01	0.256 ± 0.06	0.03 ± 0.01	0.68 ± 0.04	0.00 ± 0.01
7.5 min	0.03 ± 0.03	0.03 ± 0.01	0.273 ± 0.05	0.03 ± 0.01	0.75 ± 0.05	0.00 ± 0.01
15 min	0.08 ± 0.04	0.02 ± 0.01	0.248 ± 0.05	0.03 ± 0.01	0.68 ± 0.04	0.00 ± 0.01

Data presented as mean ± standard deviation.

instant effect was also calculated using the formula: surviving fraction $= e^{-(\alpha D + \beta D^2)}$ for each dose, *i.e.* the effect when the dose was delivered in a single irradiation by the treatment beam (400 MU min^{-1}). As a comparison, the generated surviving fraction data for the split-dose treatments were used to calculate the protracted effective dose for each dose point, *i.e.* the dose required to cause the same level of cell kill if the dose was delivered in a single fraction.

The calculated surviving fractions for imaging-to-treatment times of 7.5 and 15 min for DU-145, H460 and AGO-1552b cells are presented in Table 4. The data were subsequently plotted and fitted using the linear quadratic model, although data were not presented as overlaid curves. The theoretical results are in good agreement with the experimental data presented previously. Currently, dose incorporation is rarely implemented owing to the practical difficulties of calculating imaging dose and summing this with the treatment dose, as well as the uncertainty of repeat exposures during treatment to ensure set-up accuracy. Hence, the modelling was used to determine the effect of not incorporating the dose into the plan. Table 5 shows that the protracted effective dose was lower only than the prescribed instant effect for the DU-145 cells delivering 8 Gy.

DISCUSSION

In the era of high-precision conformal and adaptive radiotherapy, the use of imaging in the treatment room is set to increase. Since the dose received from pre-treatment verification imaging can be considerable,[3,8] it has been suggested that this dose should be accounted for at the treatment planning stage.[3,29,30] Although this allows for the correct calculation of normal tissue and tumour dose, imaging dose incorporation has the potential to impact the treatment efficacy in an adverse manner. This is because in the time between pre-treatment imaging and delivery of the remaining treatment dose, sublethal damage repair may occur,[31] which may lead to a reduced amount of sublethal damage that can be subsequently compounded to lethal damage by the treatment dose. In turn, this has the potential to result in an increase in the surviving fraction of cells after treatment.

The aim of this research was to investigate the impact of imaging dose incorporation on cell survival *in vitro*, in both human cancer and normal tissue cell lines. The results from the experimental studies presented here reveal that imaging dose incorporation has no significant impact on cell survival, for clinically relevant imaging-to-treatment times of 7.5 or 15 min for all cell lines investigated. Results from DU-145 cells support the results from related studies by Butterworth et al[32] and McGarry et al,[33] who reported no statistically significant trends towards increased cell survival in DU-145 cells for prolonged treatment delivery times. AGO-1522b cells have shown some dose rate effects for non-modulated beams,[33] but no effects were observed in this study. The results for H460 cells are in clear disagreement with the preliminary experimental findings of Yang et al[10] who reported a 12.6% ($p < 0.02$) increase in cell survival when a 5-cGy pre-treatment imaging dose was delivered to the cells prior to the delivery of a therapeutic dose of 200 cGy. However, the details of the experimental protocol used and specific results of this study by Yang et al[10] remain unpublished. Bewes et al[34] investigated the impact of prolonged treatment delivery times on cell survival. They reported that as the time taken to deliver a specified dose of radiation increased, a corresponding increase in cell survival was observed for a melanoma cell line (MM576) and for H460 cells. The study by Bewes et al[34] highlights that extended treatment times may significantly impact tumour control in an adverse manner; however, these experiments were undertaken for continuous dose irradiation, whereas the study reported herein is for a split-dose irradiation scenario.

The experimental data presented for AGO-1522b, DU-145 and H460 cells were found to be in excellent agreement with the theoretically determined data, which was modelled using the Lea–Catcheside dose protraction factor.[9,23] These results are encouraging, as the imaging-to-treatment times used are of clinical relevance. Furthermore, in terms of effective dose (*i.e.* the dose required to achieve the same level of cell kill if the dose was delivered in a single irradiation), the largest percentage difference was found to be 1.37%. From both the experimental and theoretical data presented here, incorporation of an imaging dose of 5 cGy with a prescribed treatment dose, for imaging-to-treatment times not exceeding 15 min, would not be expected to impact tumour control in an adverse manner since no significant change in cell survival is observed. These findings are in agreement with the theoretical study of Flynn[9] who reported that the loss of radiobiological efficiency due to sublethal damage repair, when imaging doses are incorporated with the treatment dose, is clinically insignificant if the imaging dose delivered is ≤5% of the total dose, or if the delay time between imaging and treatment is in the order of 5 min.

Although sublethal damage repair is a key player in the context of the research presented here, other biological effects such as adaptive responses and bystander effects may become more influential as radiotherapy techniques and delivery options become more sophisticated.[17]

Table 4. Instant *vs* protracted effect for DU-145, H460 and AGO-1522b cells incorporating the dose into the plan.

$\tau_{I-T} = 7.5$ min								
Instant effect dose	Imaging dose (Gy)	Treatment dose (Gy)	DU-145		H460		AGO-1522b	
			Protracted effective dose	Difference (%)	Protracted effective dose	Difference (%)	Protracted effective dose	Difference (%)
1	0.05	0.95	–	–	–	–	1.00	0.00
2	0.05	1.95	1.99	−0.52	2.00	−0.06	2.00	0.00
4	0.05	3.95	3.97	−0.70	4.00	−0.10	4.00	−0.01
8	0.05	7.95	7.90	−1.27	7.98	−0.19	–	–
$\tau_{I-T} = 15$ min								
Instant effect dose	Imaging dose (Gy)	Treatment dose (Gy)	DU-145		H460		AGO-1522b	
			Protracted effective dose	Difference (%)	Protracted effective dose	Difference (%)	Protracted effective dose	Difference (%)
1	0.05	0.95	–	–	–	–	1.00	−0.01
2	0.05	1.95	1.98	−0.76	2.00	−0.11	2.00	−0.01
4	0.05	3.95	3.97	−0.86	3.99	−0.13	4.00	−0.01
8	0.05	7.95	7.89	−1.37	7.98	−0.21	–	–

τ_{I-T}, imaging-to-treatment time.

Table 5. Instant *vs* protracted effect for DU-145, H460 and AGO-1522b cells without incorporating the dose into the plan.

$\tau_{I-T} = 7.5$ min								
Instant effect dose	Imaging dose (Gy)	Treatment dose (Gy)	DU-145		H460		AGO-1522b	
			Protracted effective dose	Difference (%)	Protracted effective dose	Difference (%)	Protracted effective dose	Difference (%)
1	0.05	1	–	–	–	–	1.00	0.06
2	0.05	2	2.01	0.73	2.01	0.74	2.00	0.06
4	0.05	4	4.00	0.13	4.02	0.51	4.00	0.06
8	0.05	8	7.94	−0.79	8.02	0.22	–	–
$\tau_{I-T} = 15$ min								
Instant effect dose	Imaging dose (Gy)	Treatment dose (Gy)	DU-145		H460		AGO-1522b	
			Protracted effective dose	Difference (%)	Protracted effective dose	Difference (%)	Protracted effective dose	Difference (%)
1	0.05	1	–	–	–	–	1.00	0.06
2	0.05	2	2.01	0.48	2.01	0.70	2.00	0.06
4	0.05	4	4.00	−0.05	4.02	0.48	4.00	0.05
8	0.05	8	7.93	−0.88	8.02	0.19	–	–

τ_{I-T}, imaging-to-treatment time.

Extrapolation of these *in vitro* and theoretical findings to the clinical context is restricted owing to the limitations of two-dimensional cell culture methods, which do not replicate the vascular architecture of complex tumours. In addition, the fact that only megavoltage imaging beams were used in this study may limit the applicability of the results to other types of verification imaging. However, the preliminary megavoltage dose represents a portal imaging dose, which is on the higher side of the doses received by image-guided radiotherapy. Delivering CBCT or even paired images from different directions will result in non-homogenous (non-uniform) doses across organs or cells.[3] This could be complicated further by differences in dose deposition from kilovoltage imaging compared with megavoltage imaging and other factors such as patient dimensions and the treatment site. Although all of these factors cannot be taken into account, it is important to study the effects with a known uniform dose, delivered in a controlled fashion, before further investigation into this complex area of radiotherapy. With such a paucity of data in the literature on imaging effects, the novel work presented here provides a framework for further study.

CONCLUSIONS

For DU-145, H460 and AGO-1522b cells, incorporation of an imaging dose of 5 cGy with the prescribed treatment dose was not found to have a significant impact on cell survival, for clinically relevant imaging-to-treatment times of 7.5 or 15 min. These findings were in good agreement with theoretically modelled data, based on the Lea–Catcheside dose protraction factor. These data suggest that imaging dose incorporation should not be expected to impact on tumour control in an adverse manner, since no significant increase in cell survival was observed.

FUNDING

This work was supported by grants from Cancer Research UK [grant numbers: C1513/A7047 (KMP), C212/A11342 (SMcM, ARH) and C212/A12463 (AJC)].

ACKNOWLEDGMENTS

The authors wish to acknowledge financial support from Cancer Research UK. The authors also wish to acknowledge the help of Dr Denise Irvine.

REFERENCES

1. Nijkamp J, Pos FJ, Nuver TT, de Jong R, Remeijer P, Sonke JJ, et al. Adaptive radiotherapy for prostate cancer using kilovoltage cone-beam computed tomography: first clinical results. *Int J Radiat Oncol Biol Phys* 2008; **70**: 75–82.
2. Mell LK, Mehrotra AK, Mundt AJ. Intensity-modulated radiation therapy use in the U.S., 2004. *Cancer* 2005; **104**: 1296–303. doi: 10.1002/cncr.21284
3. Stock M, Palm A, Altendorfer A, Steiner E, Georg D. IGRT induced dose burden for a variety of imaging protocols at two different anatomical sites. *Radiother Oncol* 2012; **102**: 355–63. doi: 10.1016/j.radonc.2011.10.005
4. Dawson LA, Jaffray DA. Advances in image-guided radiation therapy *J Clin Oncol* 2007; **25**: 938–46. doi: 10.1200/JCO.2006.09.9515
5. Little MP, Wakeford R, Tawn EJ, Bouffler SD, Berrington de Gonzalez A. Risks associated with low doses and low dose rates of ionizing radiation: why linearity may be (almost) the best we can do. *Radiology* 2009; **251**: 6–12. doi: 10.1148/radiol.2511081686
6. Harrison RM, Wilkinson M, Shemilt A, Rawlings DJ, Moore M, Lecomber AR. Organ doses from prostate radiotherapy and associated concomitant exposures. *Br J Radiol* 2006; **79**: 487–96. doi: 10.1259/bjr/16187818
7. Fazel R, Krumholz HM, Wang Y, Ross JS, Chen J, Ting HH, et al. Exposure to low-dose ionizing radiation from medical imaging procedures. *N Engl J Med* 2009; **361**: 849–57. doi: 10.1056/NEJMoa0901249
8. Spezi E, Downes P, Jarvis R, Radu E, Straffurth J. Patient-specific three-dimensional concomitant dose from cone beam computed tomography exposure in image-guided radiotherapy. *Int J Radiat Oncol Biol Phys* 2012; **83**: 419–26.
9. Flynn RT. Loss of radiobiological effect of imaging dose in image guided radiotherapy due to prolonged imaging-to-treatment times. *Med Phys* 2010; **37**: 2761–9.
10. Yang W, Wang L, Read P, Larner J, Sheng K. Increased tumor radioresistance by imaging doses from volumetric image guided radiation therapy. *Med Phys* 2009; **36**: 2808.
11. Tapio S, Jacob V. Radioadaptive response revisited. *Radiat Environ Biophys* 2007; **46**: 1–12. doi: 10.1007/s00411-006-0078-8
12. Prise KM, Folkard M, Michael BD. Radiation-induced bystander and adaptive responses in cell and tissue models. *Dose Response* 2006; **4**: 263–76. doi: 10.2203/dose-response.06-113.Prise
13. Wolff S. The adaptive response in radiobiology: evolving insights and implications. *Environ Health Perspect* 1998; **106**: 277–83.
14. Sawant SG, Randers-Pehrson G, Metting NF, Hall EJ. Adaptive response and the bystander effect induced by radiation in C3H 10T(1/2) cells in culture. *Radiat Res* 2001; **156**: 177–80.
15. Prise KM, O'Sullivan JM. Radiation-induced bystander signalling in cancer therapy. *Nat Rev Cancer* 2009; **9**: 351–60. doi: 10.1038/nrc2603
16. Bonner WM. Low-dose radiation: thresholds, bystander effects, and adaptive responses. *Proc Natl Acad Sci U S A* 2003; **100**: 4973–5. doi: 10.1073/pnas.1031538100
17. Butterworth KT, McMahon SJ, Hounsell AR, O'Sullivan JM, Prise KM. Bystander signalling: exploring clinical relevance through new approaches and new models. *Clin Oncol (R Coll Radiol)* 2013; **13**: 586–92. doi: 10.1016/j.clon.2013.06.005
18. Shadley JD, Wolff S. Very low doses of X-rays can cause human lymphocytes to become less susceptible to ionizing radiation. *Mutagenesis* 1987; **2**: 95–6.
19. Fowler JF, Welsh JS, Howard SP. Loss of biological effect in prolonged fraction delivery. *Int J Radiat Oncol Biol Phys* 2004; **59**: 242–9. doi: 10.1016/j.ijrobp.2004.01.004
20. Wang JZ, Li XA, D'Souza WD, Stewart RD. Impact of prolonged fraction delivery times on tumor control: a note of caution for intensity-modulated radiation therapy (IMRT). *Int J Radiat Oncol Biol Phys* 2003; **57**: 543–52.
21. Wang JZ, Guerrero M, Li XA. How low is the alpha/beta ratio for prostate cancer. *Int J Radiat Oncol Biol Phys* 2003; **55**: 194–203.
22. Morgan WF, Naqvi SA, Yu C. Does the time required to deliver IMRT reduce its biological effectiveness? *Int J Radiat Oncol Biol Phys* 2002; **54**: 222.
23. Lea DE, Catcheside DG. The mechanism of the induction by radiation of chromosome

aberrations in *Tradescantia*. *J Genet* 1942; **44**: 216–45.
24. Puck TT, Marcus PI. Action of x-rays on mammalian cells. *J Exp Med* 1956; **103**: 653–66.
25. McGarry CK, Grattan MW, Cosgrove VP. Optimization of image quality and dose for Varian aS500 electronic portal imaging devices (EPIDs). *Phys Med Biol* 2007; **52**: 6865–77. doi: 10.1088/0031-9155/52/23/006
26. IPSM. Code of practice for high-energy photon therapy dosimetry based on the NPL absorbed dose calibration service. *Phys Med Biol* 1990; **35**: 1355–60.
27. Schmitt JD, Warren GW, Wang IZ. Potential increase in biological effectiveness from field timing optimization for stereotactic body radiation therapy. *J Exp Med* 2012; **39**: 2956–63. doi: 10.1118/1.4709605
28. Kavanagh JN, Currell FJ, Timson DJ, Savage KI, Richard DJ, McMahon SJ, et al. Anti-proton induced DNA damage: proton like in flight, carbon-ion like near rest. *Sci Rep* 2013; **3**: 1770. doi: 10.1038/srep01770
29. Morin O, Gillis A, Descovich M, Chen J, Aubin M, Aubry JF, et al. Patient dose considerations for routine megavoltage conebeam CT imaging. *Med Phys* 2007; **34**: 1819–27.
30. Miften M, Gayou O, Reitz B, Fuhrer R, Leicher B, Parda DS. IMRT planning and delivery incorporating daily dose from mega-voltage cone-beam computed tomography imaging. *Med Phys* 2007; **34**: 3760–7.
31. Ward JF. Mechanisms of DNA repair and their potential modification for radiotherapy. *Int J Radiat Oncol Biol Phys* 1986; **12**: 1027–32.
32. Butterworth KT, McGarry CK, Trainer C, McMahon SJ, O'Sullivan JM, Schettino G, et al. Dose, dose-rate and field size effects on cell survival following exposure to non-uniform radiation fields. *Phys Med Biol* 2012; **57**: 3197–206. doi: 10.1088/0031-9155/57/10/3197
33. McGarry CK, Butterworth KT, Trainor C, O'Sullivan JM, Prise KM, Hounsell AR. Temporal characterization and *in vitro* comparison of cell survival following the delivery of 3D-conformal, intensity-modulated radiation therapy (IMRT) and volumetric modulated arc therapy (VMAT). *Phys Med Biol* 2011; **56**: 2445–57.
34. Bewes JM, Suchowerska N, Jackson M, Zhang M, McKenzie DR. The radiobiological effect of intra-fraction dose-rate modulation in intensity modulated radiation therapy (IMRT). *Phys Med Biol* 2008; **53**: 3567–78. doi: 10.1088/0031-9155/53/13/012